International Journal on Mechanical Engineering and Robotics

ISSN: 2321-5747

Volume 11 Issue 1 (2022) | Pages: 6-16

Design, Analysis, and Experimental Evaluation of an Off-Grid Solar Photovoltaic Electric Vehicle Charging Infrastructure Incorporating Lithium-Ion Energy Storage Systems

Mohsin I. Shaikh[1], Monesh R. Kshirsagar[2], Ashish V. Narsale[3], Rahul T. Umap[4], Vishal Meshram[5*]

[1,2,3,4,5]Department of Mechanical Engineering, Shree Chanakya Education Society's Indira College of Engineering and Management, Parandwadi, Savitribai Phule Pune University, Pune, Maharashtra, India

Corresponding Author: vishalam85@gmail.com

Peer Review Information

Type: *Article*
Received: *16 April 2022*
Revised: *12 May 2022*
Accepted: *15 June 2022*
Published: *05 July 2022*

Abstract

The rapid global transition toward Electric Vehicles (EVs) aims to mitigate greenhouse gas emissions and dependency on fossil fuels. However, reliance on non-renewable grid power for EV charging transfers environmental burdens back to conventional power plants. This study presents the design, structural analysis, and experimental performance evaluation of a portable, off-grid solar photovoltaic (PV) EV charging station featuring advanced Lithium-ion battery storage integrated with a Battery Management System (BMS). A mechanical frame structure fabricated from Plain Carbon Steel was designed to support the 60 W polycrystalline solar array and integrated electronic assemblies. Finite Element Analysis (FEA) performed in SolidWorks Simulation demonstrated structural integrity under operational static loading, exhibiting a maximum von Mises stress of 1.708×10^7 N/m^2, a peak resultant displacement of 0.3658 mm, and a minimum Factor of Safety (FOS) of 12.92. Experimental charging and discharging trials conducted on the standalone energy storage system demonstrated effective charge regulation, voltage conversion via step-up/step-down converters, and operational reliability. The total bill of materials cost for the functional prototype was evaluated at ₹21,770. The proposed system provides a decentralized, sustainable solution for campus mobility and public parking facilities.

Keywords: Solar Photovoltaic; Electric Vehicle Charging Station; Off-Grid Power System; Lithium-ion Battery; Battery Management System; Finite Element Analysis.

How to Cite This Article

Shaikh, M. I., Kshirsagar, M. R., Narsale, A. V., Umap, R. T., & Meshram, V. (2022). Design, analysis, and experimental evaluation of an off-grid solar photovoltaic electric vehicle charging infrastructure incorporating lithium-ion energy storage systems. *International Journal on Mechanical Engineering and Robotics,* 11(1), 6-16.

Introduction

Solar energy conversion remains one of the primary avenues in renewable energy research. Solar radiation is converted primarily into thermal or electrical energy, with photovoltaic systems finding applications across rural electrification, water pumping, satellite communications, and grid-tied or stand-alone power plants. Rapid population expansion and economic growth have accelerated fossil fuel depletion and intensified environmental concerns regarding greenhouse gas emissions. Modern technological automation increases overall electronic device reliance, elevating global energy consumption demands.

Transitioning transportation sectors toward electrification offers a viable strategy for reducing vehicle emissions. However, charging EVs using grid power produced by conventional thermal power plants fails to achieve complete decarbonization. Standalone solar-powered EV charging stations present an effective infrastructure model to decouple EV charging from fossil-fuel-dominated power grids.

Off-grid solar charging stations, also known as autonomous EV chargers, utilize solar PV arrays to feed localized energy storage systems, which subsequently power vehicle chargers without local grid connectivity. This independent architecture allows deployment in remote locations, public parking spaces, and educational campuses. This study designs and evaluates a mobile off-grid solar EV charging system equipped with a Lithium-ion storage battery pack, integrated BMS, charge controller, and power-conditioning step-up/step-down converters.

Literature Review

Integration of solar PV generation with EV charging systems has been widely investigated. Research on solar EV chargers demonstrates that DC-DC boost converters using Maximum Power Point Tracking (MPPT) optimize PV array output voltage to station battery banks, while buck converters step down station voltages to vehicle battery levels using constant-current/constant-voltage (CC/CV) protocols. Coordinated power management among utilities, solar PV generation, and local energy reserves reduces peak demand penalties and minimizes grid harmonic distortion.

Linear programming models applied to shared solar-powered EV charging infrastructure have shown that matching PV array capacities to parking lot dimensions maximizes self-consumption and customer satisfaction in car-sharing fleets. Dynamic charging profiles, such as Gaussian charging algorithms combined with local storage sizing, mitigate distribution grid congestion compared to standard constant-power charging.

Renewable EV charging research spans four primary domains:

1. Powering EVs in isolated/rural regions far from central grids.
2. Mitigating grid overloading through PV-shaded parking structures.
3. PV micro-grid architectures utilizing second-life EV batteries for localized buffer storage.
4. Vehicle-to-Grid (V2G) bi-directional power exchange models balancing intermittent generation.

Research Gap

While theoretical models and simulation studies for solar-assisted charging infrastructure exist extensively in literature, physical prototyping and experimental operational characterization of compact, highly mobile off-grid EV charging stations remain limited. Furthermore, direct comparisons between traditional Lead-Acid battery performance and high-density Lithium-ion battery packs with active BMS balancing under real ambient charging-discharging conditions require experimental validation.

Novelty

This work delivers a complete end-to-end design, structural simulation, physical fabrication, and real-world experimental characterization of a multi-voltage portable off-grid solar EV charging unit. Key novel aspects include:

- Integration of a multi-directional structural solar panel frame fabricated from Plain Carbon Steel with verified FEA structural integrity.
- Implementation of a high-density 18650-based Lithium-ion battery pack regulated by a 4S 40A BMS for cell balancing and overcurrent/short-circuit protection.
- Dual step-up and step-down DC-DC power converter topologies enabling flexible power delivery for 3-wheeled campus EVs, small electronic equipment, and mobile devices.

Objectives

1. Design and manufacture a working prototype of an off-grid solar-powered charging station for EV battery charging.
2. Perform structural strength and factor-of-safety analysis on the supporting structural frame using FEA tools.

3. Conduct component selection and real-world performance characterization across charging and discharging cycles using different energy storage technologies (Lead-Acid and Lithium-ion).

Materials and Methods

System Architecture

The system operational flow is depicted in Fig. 1. Solar irradiance incident on the photovoltaic array generates DC electricity, which is routed through an MPPT solar charge controller to charge the main Lithium-ion energy storage pack. Dual directional Light Dependent Resistors (LDRs) positioned along North-South axes provide directional sensing to adjust the solar panel tilt motor toward peak solar intensity. Dual DC-DC converters (step-up and step-down) regulate output terminals to match specific vehicle battery voltages.

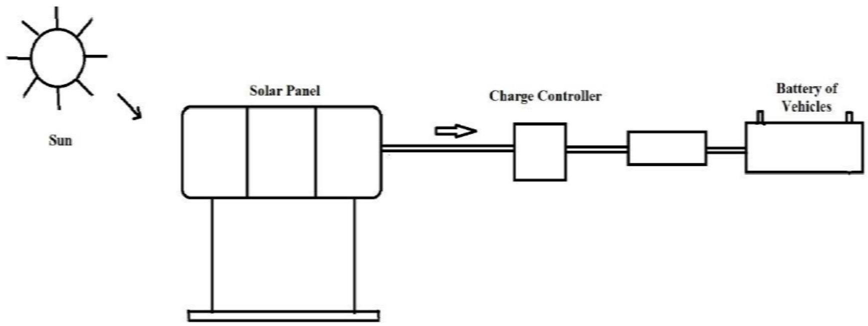

Fig. 1. *Block diagram of the off-grid solar electric vehicle charging station.*

Structural Frame Construction

The supporting chassis and structural framework were constructed using Mild Steel / Plain Carbon Steel. Plain Carbon Steel was selected due to its high tensile strength, economic availability, ease of machinability/weldability, and low thermal expansion coefficient. The mechanical frame supports the vertical pulleys, sprockets, solar panel assembly, battery pack, and electronic control box. The fabricated physical frame structure is shown in Fig. 2.

Fig. 2. *Fabricated Plain Carbon Steel frame structure.*

System Components and Specifications

Solar Charge Controller

A 12V, 10A/ 15A MPPT solar charge controller protects the battery pack from overcharging by continuously monitoring voltage levels. As shown in Fig. 3, the unit regulates power transmission across three primary charging phases: bulk stage (charging up to 80% capacity), absorption stage (current reduction near full capacity), and float stage (trickle charge maintenance).

Fig. 3. *MPPT solar charge controller unit.*

Lithium-Ion Battery Pack and Cells

The primary storage system utilizes cylindrical 18650 Lithium-ion cells. The dimensional parameters and cell configuration are illustrated in Fig. 4, with individual cell specs as follows:

- Dimensions: 18 mm diameter × 65mm height
- Weight: 45 g
- Nominal Voltage: 3.7V
- Charging Cut-Off Voltage: 4.2V
- Discharging Cut-Off Voltage: 3.0V
- Nominal Capacity: 1500 mAh (5.55 Wh)
- Maximum Charge / Discharge Current: 0.5C / 1C

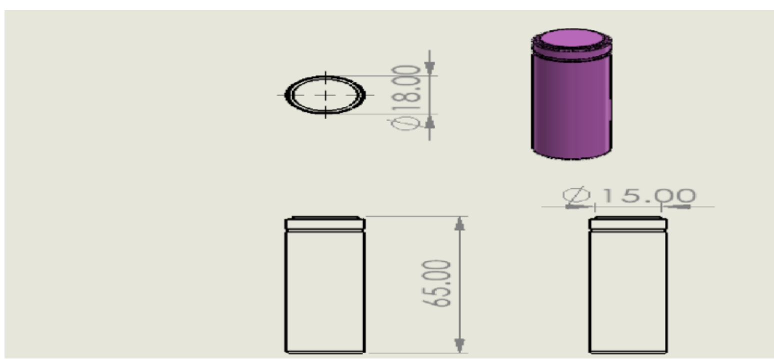

Fig. 4. *Technical specification and dimensions of 18650 Li-ion cell.*

Cells are arranged in a series-parallel modular configuration to form a 15V, 19Ah station battery pack, as shown in Fig. 5.

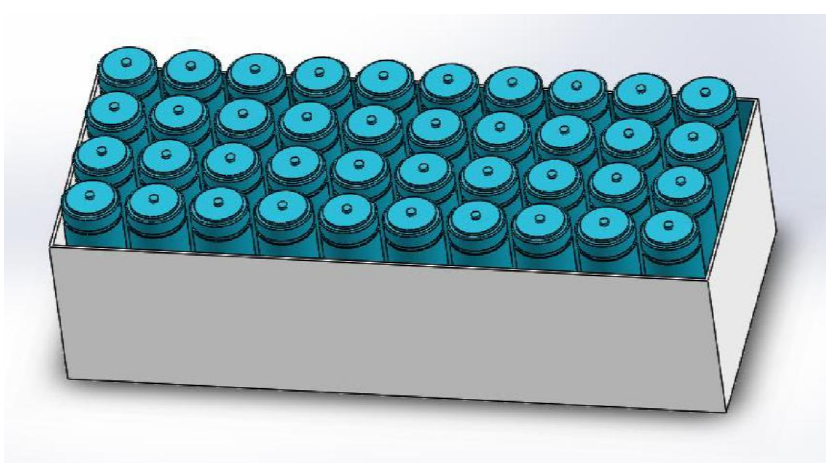

Fig. 5. *Assembled Lithium-ion battery pack.*

Photovoltaic Solar Panel

The station utilizes a polycrystalline solar PV module as pictured in Fig. 6. The technical output specifications under standard test conditions comprise:

- Maximum Rated Power Output: 60W
- Peak Voltage Output: 10 V – 18 V
- Rated Current: 0.5 A – 3.5 A

Fig. 6. *Polycrystalline solar panel module.*

Battery Management System (BMS)

A 4S 40A solid-state BMS board (Fig. 7) is integrated directly onto the battery pack. The BMS provides passive cell balancing, overcurrent protection, overvoltage cut-off, short-circuit isolation, and under-voltage protection.

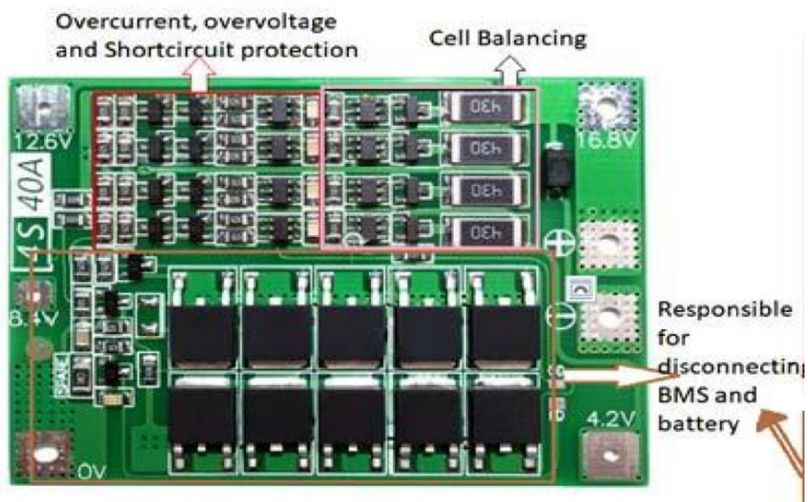

Fig. 7. *4S 40A Battery Management System circuit board.*

Step-Up DC-DC Boost Converter

To step up module voltages to match higher vehicle battery terminals, a step-up boost converter (Fig. 8) is installed.

- Input Voltage Range: 10 V - 60 V
- Maximum Input Current: 15 A
- Output Voltage Range: 12 V - 80 V (continuously adjustable)
- Maximum Output Current: 10 A
- Peak Conversion Efficiency: Up to 95%
- Mass: 251 g

Fig. 8. *High-power step-up DC-DC boost converter module.*

Step-Down DC-DC Buck Converter

For low-voltage auxiliary charging and device power delivery, an XL4016 PWM-modulated step-down buck converter (Fig. 9) is incorporated.

- Supply Input Voltage: 4 V - 40 V
- Output Voltage Range: 1.25 V - 36 V
- Maximum Output Current: 8 A (5 A continuous without forced cooling)
- Peak Power Rating: 200 W
- Switching Frequency: 180 kHz
- Peak Conversion Efficiency: 94%

Fig. 9. *XL4016 PWM step-down DC-DC buck converter module.*

Mathematical Modelling & Governing Equations

The total effective electrical power transferred through the conversion modules is governed by:

$$P = V \cdot I$$

where P is power in Watts, V is input DC voltage in Volts, and I is operating current in Amperes.

Linear elastic structural response within the supporting frame under static loading is formulated using standard isotropic Hooke's Law relations:

$$\sigma_{ij} = C_{ijkl} \cdot \varepsilon_{kl}$$

Where, σ_{ij} represents the stress tensor, ε_{kl} is the strain tensor, and C_{ijkl} is the elastic stiffness tensor defined by Young's Modulus € and Poisson's Ratio (ν). Equivalent von Mises stress (σ_{vm}) evaluated across the frame nodes is defined as:

$$\sigma_{vm} = \sqrt{\frac{1}{2}\left[\left(\sigma_x - \sigma_y\right)^2 + \left(\sigma_y - \sigma_z\right)^2 + (\sigma_z - \sigma_x)^2 + \left(\tau_{xy}^2 + \tau_{yz}^2 + \tau_{zx}^2\right)\right]}$$

The minimum Factor of Safety (FOS) is calculated relative to the material yield strength (σ_y):

$$FOS = \frac{\sigma_y}{\sigma_{vm,max}}$$

FEA CAD Modeling & Numerical Simulation Setup

The complete 3D assembly model of the mobile charging station was developed in SolidWorks 2022. Isometric, top, and dimensional drafting views are provided in Fig. 10 and Fig. 11.

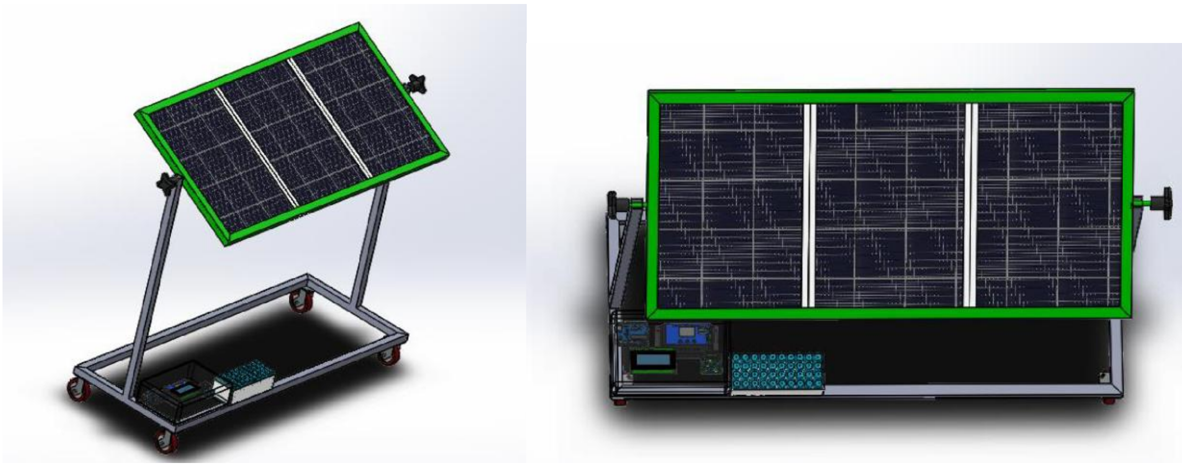

Fig.10. *CAD solid model of the assembled solar charging station (Isometric and Top view).*

Material Properties

The mechanical framework uses Plain Carbon Steel. Table I outlines the isotropic material parameters applied in the FEA simulation environment.

Table 1. *Mechanical and Physical Properties of Plain Carbon Steel*

Property Parameter	**Value**	**Unit**
Model Type	Linear Elastic Isotropic	—
Default Failure Criterion	Max von Mises Stress	—
Yield Strength (σ_y)	2.20594×10^8	N/m^2
Ultimate Tensile Strength (σ_u)	3.99826×10^8	N/m^2
Elastic Modulus (E)	2.10000×10^{11}	N/m^2
Poisson's Ratio (ν)	0.28	Dimensionless
Mass Density (ρ)	7800	kg/m^3
Shear Modulus (G)	7.90000×10^{10}	N/m^2
Thermal Expansion Coefficient (α)	1.30000×10^{-5}	K^{-1}

Simulation Results & Strength Analysis

Static FEA analysis was executed under full gravity and operational loading conditions. The maximum von Mises stress plots and resultant displacement distributions are shown in Fig. 12 and Fig. 13, with critical values compiled in Table II.

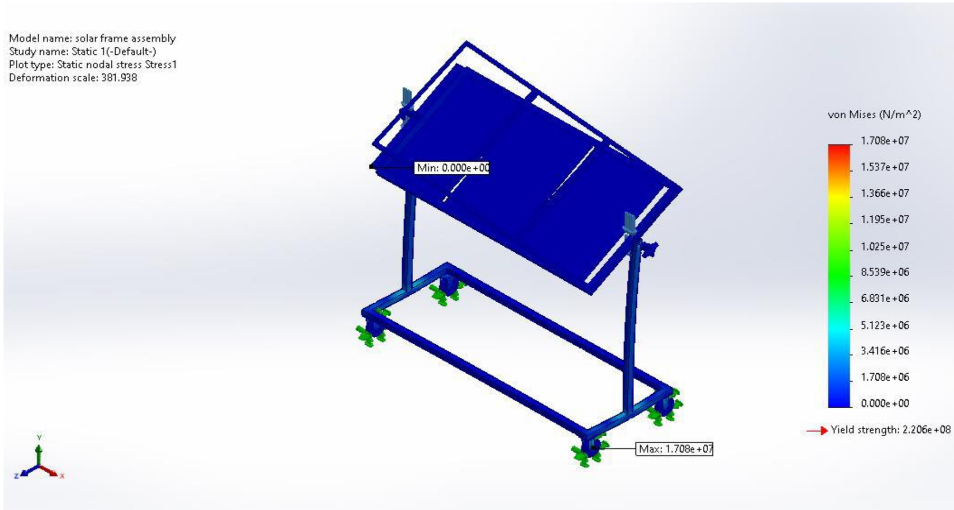

Fig. 11. *FEA stress and displacement contour plots of solar frame assembly.*

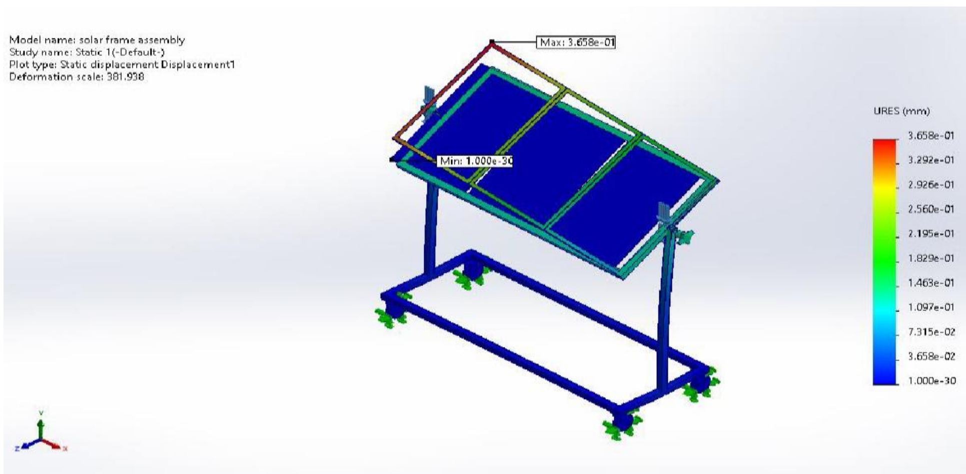

Fig. 12. *Factor of Safety (FOS) distribution contour plot of solar frame assembly.*

Table 2. *Finite Element Analysis Numerical Results*

Study Metric	**Minimum Value**	**Maximum Value**	**Critical Node**
von Mises Stress (σ_{vm})	0.000×10^0 N/m^2	1.708×10^7 N/m^2	Node 19352
Resultant Displacement (U_{res})	0.000 mm	0.3658 mm	Node 1765
Factor of Safety (FOS)	12.92	1.000×10^{16}	Node 19352

The minimum FOS of 12.92 occurs at Node 19352, confirming that the structural framework easily withstands maximum operational loads without risk of yielding or permanent deformation.

Experimental Results and Discussion

Real-world operational charging and discharging trials were conducted on the manufactured solar charging prototype. The recorded data across different trial dates is summarized in Table III.

Table 3. *Experimental Charging, Discharging, and Auxiliary Mobile Charging Test Data*

Trial Set	**Date**	**Process Mode**	**Time**	**Battery State / Level (%)**	**Terminal Voltage (V)**
Set 1	21/04/2023	Solar Charging	1:00 PM	18%	—

		Solar Charging	2:00 PM	30%	—
		Solar Charging	3:00 PM	45%	—
		Solar Charging	4:00 PM	55%	—
Set 2	11/05/2023	Station Discharging	12:10 PM	54%	12.50 V
		Station Discharging	1:10 PM	45%	11.57 V
		Station Discharging	2:10 PM	33%	10.50 V
		Station Discharging	3:10 PM	10%	9.00 V
Set 3	12/05/2023	Fast Solar Charging	12:15 PM	—	10.00 V
		Fast Solar Charging	12:45 PM	75%	12.00 V
		Fast Solar Charging	1.02 PM	78%	—
		Fast Solar Charging	1:15 PM	82%	—
		Fast Solar Charging	1:22 PM	84%	—
Set 4	12/05/2023	Mobile Device Charging	12:57 PM	26%	—
		Mobile Device Charging	1:00 PM	27%	—
		Mobile Device Charging	1:07 PM	28%	—
		Mobile Device Charging	1:12 PM	29%	—
		Mobile Device Charging	1:18 PM	30%	—

Charging Performance Analysis

During the primary charging trial (21/04/2023), the battery charge state increased linearly from 1% at 1:00 PM to 55% at 4:00 PM under steady solar irradiance. During peak solar radiation on 12/05/2023, the fast solar charging mode rapidly replenished the storage pack from 10.0 V to 12.0 V (75% state-of-charge) within 30 minutes, reaching 84% capacity by 1:22 PM.

Discharging & Auxiliary Output Evaluation

During discharging trials (11/05/2023), terminal voltage dropped predictably from 12.5 V(54% capacity) at 12:10 PM to 9.0V (10% cut-off) at 3:10 PM under sustained vehicle load. Concurrent auxiliary trials verified stable 5 V step-down buck conversion for mobile devices, raising a smartphone battery from 26% to 30% in 21 minutes without perturbing main bus stability.

Regulatory Guidelines for Charging Infrastructure

Compliance with public charging infrastructure guidelines is vital for commercial scalability. Standard regulatory specifications mandate:

1. Fast Charging Requirements: High-power long-distance EV charging stations require at least two ≥ 100 kW chargers (200-1000 V) supporting CCS and CHAdeMO standards with liquid-cooled cabling.
2. Station Density Requirements: Public charging stations should be spaced within a 3 km×3 km grid in urban settings, and every 25 km along both sides of highways. Fast charging stations for heavy-duty vehicles require 100 km highway spacing.
3. Tariff Structures: Electricity tariffs for public EV charging stations are capped by regulatory commissions at average cost of supply plus a maximum 15% margin.

Economic Cost Analysis

The total production cost for the functional portable prototype is detailed in Table IV.

Table 4. *Bill of Materials and Fabrication Cost Estimation*

Sr no	**Part Name**	**Material**	**Qty**	**Cost**
1.	Solar Panels Poly crystalline 60 watt	PV	1 No	5000
2.	Battery 15 V, 19 Amp	Lithium Ion	1 No	4500
3.	BMS	Std	1 No	650

4.	Charge controller 12 V, 10 Amp	Std	1 No	900
5.	Step up circuit	Std	1 No	850
6.	Step down circuit	Std	1 No	350
7.	Lead Acid Battery 12V, 8 Amp	Std	1 No	900
8.	Wire 1.5 x 2 core	Std	15 m	800
9.	Wire Sleeve	Std	5 m	100
10.	Circuit Box 32 L	PVC	1 No	800
11.	Structure for Solar Panels	MS	15 Kg	2500
12.	Castor Wheels	Std	4 Nos	1600
13.	Battery Indicator	Std	1 No	1200
14.	Multimeter	Std	1 No	350
15.	Wire for Wiring 0.5 sq m	Std	10 m	80
16.	Paint	Std	0.5 L	100
17.	Nut Bolts	Std	0.5 kg	90
18.	Accessories	-	-	1000
TOTAL ESTIMATED COST				21,770/-

Sustainability, Limitations, and Future Scope

Sustainability Implications

Implementing off-grid solar EV charging stations directly decouples EV adoption from fossil-fuel-dominated power grids. Educational campuses and commercial centers adopting such systems lower their net carbon footprint, promote localized renewable energy usage, and decrease peak grid congestion.

Limitations

1. The experimental prototype utilizes a relatively small 60 W solar panel array, resulting in extended charging durations for high-capacity EV batteries.
2. Passive air cooling within the BMS limits continuous current throughput during extreme ambient thermal conditions.

Future Scope

Future iterations will incorporate active liquid cooling for high-power battery packs, larger high-efficiency monocrystalline solar arrays, automatic dual-axis sun-tracking motors, and IoT-enabled smart billing RFID systems.

Conclusion

This study successfully designed, analyzed, fabricated, and tested a portable off-grid solar-powered electric vehicle charging station. Structural analysis confirmed frame reliability with a minimum FOS of 12.92 and maximum deflection of 0.3658 mm under load. Experimental testing validated efficient power conditioning via MPPT charge control and DC converters, establishing a sustainable, low-cost platform (₹21,770) for green campus mobility and off-grid EV infrastructure deployment.

Acknowledgment

The authors acknowledge the support provided by the Department of Mechanical Engineering and the Library Department at Indira College of Engineering and Management, University of Pune.

References

1. S. C. Sheridan and C. C. Lee, "Temporal trends in absolute and relative extreme temperature events across North America," *Journal of Geophysical Research: Atmospheres*, 2018.
2. K. G. Arjun, B. G. Pruthviraj, K. Y. Chetan, and P. Rashmi, "Design and implementation of Peltier based solar powered portable refrigeration unit," in *2017 2nd IEEE International Conference on Recent Trends in Electronics, Information & Communication Technology (RTEICT)*, 2017.

3. P. G. Sonkhede and A. Pathrikar, "Portable thermoelectric refrigeration system for medical application," *International Journal of Innovative Research in Computer and Communication Engineering*, 2016.
4. D. S and A. H, "AODV Route Discovery and Route Maintenance in MANETs," in *2019 5th International Conference on Advanced Computing & Communication Systems*, 2019.
5. H. Ananda Kumar and K. Umamaheswari, "An efficient optimized handover in cognitive radio networks using cooperative spectrum sensing," *Intelligent Automation & Soft Computing*, 2017.
6. M. Suganya and H. Anandakumar, "Handover based spectrum allocation in cognitive radio networks," in *2013 International Conference on Green Computing, Communication and Conservation of Energy*, 2013.
7. M. Caramanis and J. M. Foster, "Management of electric vehicle charging to mitigate renewable generation intermittency and distribution network congestion," in *Proceedings of the 48th IEEE Conference on Decision and Control (CDC)*, 2020.
8. "Wireless Communication Using HC-05 Bluetooth Module Interface with Arduino," *International Journal of Science, Engineering and Technology Research (IJSETR)*, vol. 5, no. 4, April 2016.
9. "Development of rapid charging system for EV battery," *International Journal of Recent Technology and Engineering (IJRTE)*, vol. 7, no. 6S, March 2019.
10. "Review on Electric Vehicle, Battery Charger, Charging Station and Standards," *Research Journal of Applied Sciences, Engineering and Technology*, vol. 7, no. 2, pp. 364, 2014.